THE JOURNAL OF PHYSICAL CHEMISTRY B

Article

pubs.acs.org/JPCB

An Environmentally Sensitive Fluorescent Dye as a Multidimensional Probe of Amyloid Formation

Emma V. Yates, Georg Meisl, Tuomas P. J. Knowles,* and Christopher M. Dobson*

Department of Chemistry, University of Cambridge, Lensfield Road, Cambridge CB2 1EW, United Kingdom

Supporting Information

ABSTRACT: We have explored amyloid formation using poly(amino acid) model systems in which differences in peptide secondary structure and hydrophobicity can be introduced in a controlled manner. We show that an environmentally sensitive fluorescent dye, dapoxyl, is able to identify β-sheet structure and hydrophobic surfaces, structural features likely to be related to toxicity, as a result of changes in its excitation and emission profiles and its relative quantum yield. These results show that dapoxyl is a multidimensional probe of the time dependence of amyloid aggregation, which provides information about the presence and nature of metastable aggregation intermediates that is inaccessible to the conventional probes that rely on changes in quantum yield alone.

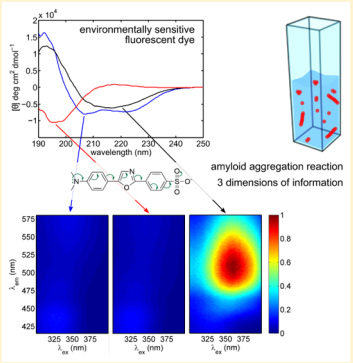

INTRODUCTION

Amyloid disorders involve the deposition of misfolded proteins in a variety of organs. In certain cases such as the systemic amyloidoses, amyloid fibrils, the stable and highly ordered end products of the aggregation process, are likely to contribute directly to pathogenesis. In other cases, notably neurodegenerative disorders including Alzheimer's and Parkinson's diseases, the oligomeric precursors to amyloid fibril formation, rather than the mature amyloid fibrils themselves, are thought to be the primary origin of toxicity and cellular damage and malfunction.[1]

Several biophysical techniques have been developed and utilized to follow the progress of amyloid fibril formation. By contrast, methods able to yield similar information about the appearance and disappearance of key intermediates in the aggregation reactions are more limited.[2] Strategies have, however, been developed for characterizing specific properties of the intermediates, although they are often destructive of the sample or proceed on a time scale which does not permit the detailed evaluation of transient species. Accordingly, attempts to define the nature and properties of intermediates have typically involved the generation of isolated populations of species that are stable enough to permit the study of their structure and toxicity by conventional biophysical methods. These efforts have revealed that oligomers with hydrophobic and β-sheet-rich conformational motifs are particularly toxic.[3−7]

Fluorescence assays have been widely used to follow the formation of amyloid fibrils. Most notably, thioflavin T (ThT) kinetic assays are a powerful and ubiquitous method for following fibril formation. These assays monitor the appearance of amyloid fibrils via an increase in the fluorescence intensity of a noncovalently bound dye;[8−11] in the majority of cases, ThT does not appear to interact significantly with early aggregation intermediates.[12−14] More recently, conjugated polyelectrolytes have been used as probes of changes in protein conformation such as those which occur during amyloid formation.[15−18] Inspired by these studies, here we explore the development of probes with similar capabilities, but which are small molecules. Indeed, in the present study we sought to deliver a new biophysical tool which can, in a single experiment, provide detailed kinetic information about the presence of mature amyloid fibrils and their associated intermediates, based on differences in secondary structure and hydrophobicity, which are particularly associated with toxicity.[3−7]

EXPERIMENTAL METHODS

Circular dichroism spectra were recorded on either a Chirascan (Applied Photophysics, Leatherhead, UK) or a Jasco (Dunmow, UK) circular dichroism spectrometer. Fluorescence data were acquired with a Cary Eclipse fluorescence spectrophotometer (Varian, Inc., Palo Alto, CA) or a FLUOstar OPTIMA plate reader (BMG Labtech, Aylesbury, UK). Poly-L-lysine hydrobromide, molecular weight 30−70 kDa (K1), poly(lysine, phenylalanine) 1:1 hydrobromide, molecular weight 20−50 kDa (K2), and thioflavin T (ThT) were purchased from Sigma (Gillingham, UK). Dapoxyl sulfonic acid, sodium salt, was purchased from Life Technologies (Warrington, UK). Bovine insulin was purchased from Seralab, (Haywards Heath, UK) or Sigma.

Prior to preparation of different secondary structural forms, K1 was dissolved in Milli-Q water, dialyzed, and lyophilized. The poly(amino acid) was then dissolved in 20 mM sodium

Received: October 2, 2015
Revised: February 10, 2016
Published: February 11, 2016

DOI: 10.1021/acs.jpcb.5b09663
J. Phys. Chem. B 2016, 120, 2087−2094

phosphate buffer at a concentration of 0.1 mg/mL, and the pH was adjusted to 7.0 to generate the extended conformer and to 11.1 to stabilize the α-helical and β-sheet conformers.[19] As described in the Supporting Information, temperatures and incubation times were varied in order to identify conditions that promoted transformation of the α-helical conformer, formed at alkaline pH at 25 °C into the β-sheet conformer; an incubation time of 60 min at 52 °C was selected as this conferred maximal conversion to the β-sheet form.

K2 as received was similarly dialyzed and lyophilized to remove counterions and likewise dissolved at 0.1 mg/mL in 20 mM sodium phosphate buffer. As described in the Supporting Information, the behavior of K2 was explored at pH values between 3.0 and 11.0, and a pH 10.0 was chosen for the system described in this paper.

The secondary structure of the samples was determined immediately following preparation. Standard parameters for the far-UV spectral measurements included irradiation at 190−250 nm, a data pitch of 0.2 nm, a scan speed of 50 nm/min, a response time of 2 s, and a bandwidth of 4 nm at a temperature of 25 °C, accumulating and averaging five spectra for each sample. Conversion of the K1 β-sheet conformer to an α-helix was found to occur when the sample was maintained at room temperature for more than 24 h. Thus, fluorescence measurements were taken immediately after preparing fresh samples of the β-sheet conformer.

Three-dimensional fluorescence spectra were acquired by measuring fluorescence emission intensity as the sample was irradiated with different excitation wavelengths, with an excitation step size of between 2 and 10 nm depending on the time resolution required for the experiment. All fluorescence measurements were carried out at 25 °C using Helma quartz fluorescence cells. The K1 fluorescence measurements were carried out by incubating 0.1 mg/mL of the α-helical, β-sheet, or extended form of K1 with 2 μM dapoxyl.

Bovine insulin was used as received. Preformed fibrils were prepared by stirring 5.0 mg/mL insulin at pH 2 and 60 °C for 20 h. The formation of fibrillar structures was confirmed by using atomic force microscopy (AFM). 0.25 mg/mL solutions of insulin fibrils were incubated with either 4 μM ThT or 4 μM dapoxyl. Stock dye concentrations were determined spectrophotometrically.

For the measurement of the kinetics of fibril formation, bovine insulin was dissolved in 50 mM NaCl buffer, pH 2.0, passed through a 0.22 μm syringe filter, and its concentration determined spectrophotometrically. Solutions were prepared at 2.0, 1.0, 0.5, 0.25, and 0.13 mg/mL. At each concentration, two samples were prepared containing insulin alone, four samples containing insulin with 4.0 μM ThT, and four samples containing insulin with 4.0 μM ThT and 4.0 μM dapoxyl. The samples were loaded onto a low-protein binding, half area 96-well assay plate (Corning, USA) and covered with aluminum sealant tape. The plate was heated at 60 °C under quiescent conditions, and ThT fluorescence was measured with 440 nm excitation and 480 nm emission filters every 120 s for 6 h.

For the three-dimensional kinetic assays, solutions of bovine insulin at concentrations varying between 0.125 and 2 mg/mL were prepared at pH 2.0 in 50 mM NaCl, and then 4 μM dapoxyl was added. The sample was heated to 60 °C under quiescent conditions, and the reaction was monitored *in situ* in a quartz fluorescence cuvette. As described above, a series of emission spectra was taken in succession at varying excitation wavelengths, and the three-dimensional spectra for specified time points were graphically reconstructed from these spectra.

Additional three-dimensional kinetic assays were performed in this manner, as described in the Supporting Information, but with AFM imaging performed in parallel at time points where the spectra suggested the presence of monomers, mature fibrils, or aggregation intermediates. Aliquots were removed from the reaction mixture at the time points indicated, diluted between 50 and 333 times, immediately deposited onto a freshly cleaved mica substrate, and allowed to dry. Samples were washed three times with Millipore water and blown dry with nitrogen. In each case the dilution chosen was the one that gave an optimal density of features on the mica slide. A low resolution image of a 100 μm × 100 μm region was acquired, so as to ensure that the regions chosen for further analysis were representative of the entire sample, and then 10 μm × 10 μm images were acquired at 1024 × 1024 pixel resolution. The scan speed was consistently set at 0.5 Hz, and gains were optimized on a sample-by-sample basis in order to follow image features in an optimal manner.

Image processing was carried out in Gwyddion.[20] A fourth-order polynomial background in the x and y dimensions was subtracted, and stripes in the fast scanning direction were normalized by matching median heights. Scars were identified and removed using automatic hardness and length thresholding, with manual corrections where necessary. The zero was set for each image analyzed by measuring several 16-pixel values on flat, featureless regions of mica in the vicinity of the image features. Their features were then automatically identified by choosing a threshold for each image that allowed collection of all the features of the image, with minimal background noise. In the case of substantial overlapping features, such as observed for clusters of fibrils, Otsu's method[21] was used. In both cases artifacts were eliminated by removing all grains identified with areas less than 6 pixels^2, followed by manual removal of any remaining artifacts. The mean height, area, projected boundary length, and maximum diameter of an inscribed disk were measured for all features. To take into account curvature, the length of each feature was estimated by dividing the area of the feature by this diameter.

RESULTS AND DISCUSSION

To model specific protein conformations in a general and highly controlled manner, we have studied a poly(amino acid) model system that enables introduction of the effects of secondary structure, hydrophobicity, and solvation. We exploit the ability of the homopolymer, poly-L-lysine (K1), to take on well-defined α-helical, β-sheet, and extended[22,23] conformations depending on the solution conditions.[24] As shown in Figure 1A, at pH 7.0, the homopolymer exists in an extended conformation, a result attributable to the electrostatic repulsion between the protonated side chains. When the pH was increased to 11.0, the α-helical conformer was observed, which converted to the β-sheet conformation upon heating for 60 min at 52 °C (Supporting Information Figure 1).[19] These conformations are typical of the α-helical, β-sheet, and random coil conformations adopted by protein chains, such that protein circular dichroism spectra are frequently interpreted using a linear combination of K1 reference spectra.[24,25] A single molecule can therefore generate all three secondary structural types, and measurements on a given sample, before and after heating, enable us to distinguish between the α-helix and β-sheet conformations.

DOI: 10.1021/acs.jpcb.5b09663
J. Phys. Chem. B 2016, 120, 2087−2094

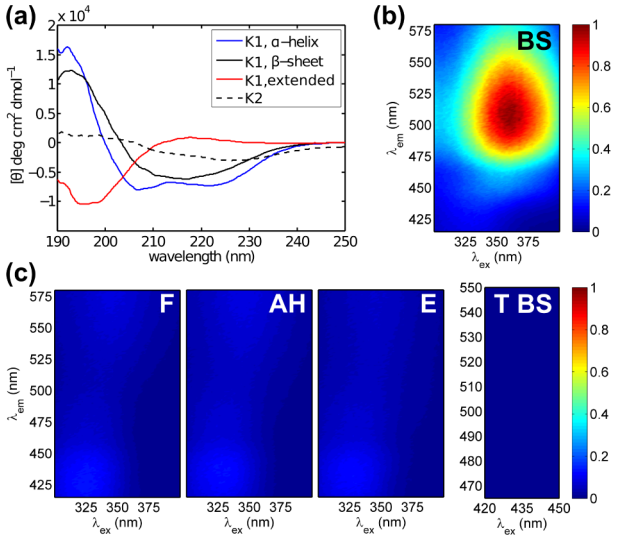

Figure 1. Secondary structural variants of poly(amino acid)s interact specifically with solvatochromic fluorescent dyes. (a) CD spectra of the hydrophilic (K1) and hydrophobic (K2) systems under different conditions reveal differences in secondary structure. (b) Interaction of dapoxyl with the β-sheet form of K1 results in a new, intense peak in the three-dimensional spectrum, which exhibits a 30-fold increase in brightness in comparison to (c) the corresponding fluorescence of dapoxyl in aqueous buffer (F), and in the presence of the α-helix (AH) and extended (E) secondary structural forms of K1. Further, the β-sheet form does not interact detectably with ThT (T BS). All spectra have been normalized relative to the peak observed for the β-sheet form (b) to highlight intensity differences.

Amyloid fibrils with cross-β-sheet structure appear to have low levels of hydration.[26] Furthermore, it has been shown that α-helical, β-sheet, and extended conformations of identical polypeptides vary in their effective hydrophobicity and compactness.[27] Specifically in the case of K1, octanol–buffer partitioning studies have indicated that the effective hydrophobicity increases significantly in the order extended < α-helix < β-sheet structures.[28] This effect has been attributed to differences in solvent hydration; the protonated side chains of the extended conformer are expected to be highly solvated. The α-helical conformer is then expected to be less highly solvated than the extended chain, both because the molecule contains fewer positive charges—as the pH is higher—and because intramolecular hydrogen bonds are formed along the polypeptide backbone. The β-sheet conformer is expected to be the least solvated due to extensive hydrogen bonding between neighboring chains.[28] Indeed, it has been estimated that in the α-helical conformation each lysine residue is hydrated by four to six water molecules, while in the β-sheet conformation each residue is predicted to be hydrated by less than two water molecules.[29]

We have prepared, in addition to K1, another species which has been chosen for its additional hydrophobicity. We examined a 1:1 copolymer of poly(lysine, phenylalanine), K2, in which phenylalanine residues are inserted into the K1 sequence at random positions. In aqueous solution, the copolymer takes on a mixture of β-sheet and extended secondary structural forms, with the composition determined by the pH. We chose pH 10, in which β-sheet secondary structure is enriched.[30] As shown in Figure 1A, the ellipticity of K2 is decreased relative to that observed for K1. This ellipticity is likely to be due to a combination of β-sheet and extended structure—alternating copolymers have been shown to be favorable for the formation of secondary structures of high purity[31]—and also distortion due to the optical activity of the phenylalanine chromophores.[30] Because of its increased hydrophobicity, K2 should be less solvated than any of the K1 structural variants.

Having established poly(amino acid) model systems where variations in secondary structure and hydrophobicity generated by changes in conditions result in differences in solvation, we examined a class of fluorescent dyes that are likely to be particularly responsive to such differences. "Push–pull" chromophores are hyperpolarizable organic molecules that have been studied primarily for their nonlinear optical properties.[32] In these fluorophores, electronic excitation corresponds to delocalization of electron density from an electron donor across a conjugated spacer to an electron acceptor, an effect that increases significantly the permanent dipole moment of the excited state relative to that of the ground state, as illustrated schematically in Figure 2. The

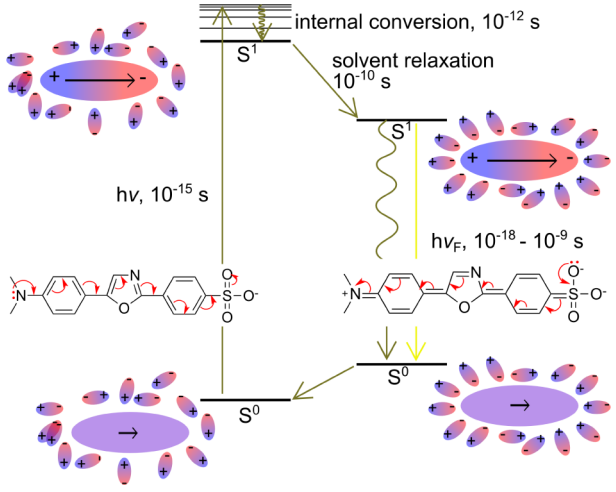

Figure 2. Solvatochromic behavior of "push–pull" chromophores (large ellipses) is shown using a Jablonski[34] diagram. Because of the rapidity of electronic transitions in comparison to nuclear motions, the initial high energy excited state (S_1) is surrounded by a ground state solvent sphere (small ellipses),[35,36] but because the excited state is long-lived relative to the time scale of solvent reorganization, the solvent sphere is able to reorganize and stabilize the excited state to an extent determined by the solvent sphere polarity. Adapted from Loving et al.[37] and showing the solvatochromic behavior of dapoxyl[38] (see later).

solvatochromic,[33] or environmentally sensitive, behavior of push–pull chromophores in particular has been noted and attributed to the molecular nonlinearity of these molecules.[32]

As shown in Figure 2, in the ground state (S^0), such a fluorescent molecule has a low permanent dipole moment, and the dipoles of the solvent sphere are randomly oriented. Following absorption of a photon with energy $h\nu$, the system rapidly undergoes a transition to an excited singlet state S^1. As illustrated for the dapoxyl structure shown, this transition corresponds to delocalization of electron density from an electron donor across the conjugated spacer to an electron acceptor; this charge separation implies that in state S^1 the fluorophore has a significantly greater permanent dipole moment than it had in state S^0. Because reorganization of atomic nuclei (10^{-10} s) requires more time than does the S^0–S^1

DOI: 10.1021/acs.jpcb.5b09663
J. Phys. Chem. B 2016, 120, 2087–2094

electronic transition (10^{-15} s), initially the first excited state is surrounded by the ground state solvent sphere.[35,36] Solvent relaxation then occurs, stabilizing the excited state and lowering its energy while raising that of the ground state. Accordingly, the energy of the fluorescence transition, $h\nu_F$, in which the permanent dipole moment of the fluorophore is lowered again through the transfer of electron density back across the conjugated spacer, is influenced by the polarity of the solvent molecules, with an increased number of polar solvent molecules reducing $h\nu_F$, thus causing a hyperchromic shift in the emission maximum. Similar solvent-dependent behavior in the excitation energy is expected, the magnitude of which will be determined by the relative stabilization of the ground and first excited states. The relative quantum yield of the fluorophores will be affected by solvent polarity and viscosity, with viscous local solvent spheres (such as hydrophobic binding pockets) reducing intramolecular twists associated with nonradiative decay pathways for the push−pull chromophores.[39−41]

In the light of these principles, we examined how the photophysical properties of a variety of push−pull fluorophores were perturbed in the presence of the α-helix, β-sheet, and extended conformers of K1 (Supporting Information Figure 3). We designed an assay in which emission spectra were acquired at a variety of excitation wavelengths, and then these composite spectra were reconstructed into a single three-dimensional spectrum that simultaneously revealed changes in excitation, emission, and relative quantum yield on interaction with each type of secondary structure.

As shown in Figures 1B and 3A,B as well as Supporting Information Figure 3, we identified one fluorophore—5-(4″-dimethylaminophenyl)-2-(4′-sulfophenyl)oxazole, dapoxyl[38]—which exhibits particularly dramatic changes in its photophysical properties in the presence of the β-sheet conformer of K1 and K2. Its chemical structure is shown in Figure 2. The corresponding spectra for free dapoxyl in aqueous buffer, and when incubated with the α-helical and extended forms of K1, are shown in plots labeled F, AH, and E respectively (Figure 1C). The 30-fold increase in relative quantum yield observed in the presence of the β-sheet conformer relative to the α-helical conformer is particularly significant, as these secondary structure forms were prepared from identical samples and under identical solution conditions, simply with and without heating. Therefore, the spectral changes observed on interaction with the K1 solution which had been heated can be entirely attributed to changes induced via interaction with the β-sheet secondary structural elements and are likely to be a result of the decrease in polarity and increase in viscosity associated with the β-sheet K1 conformer.[28]

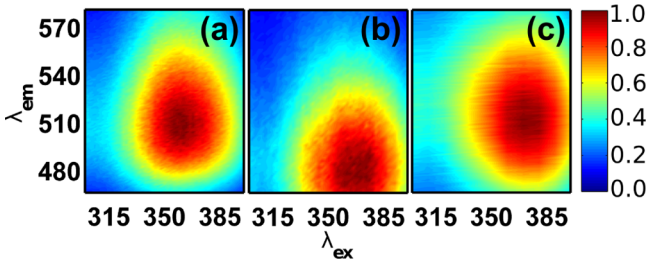

Figure 3. Three-dimensional fluorescence spectra of dapoxyl in the presence of the β-sheet forms of K1 (a) and K2 (b) and with mature insulin amyloid fibrils (c). The spectra have been normalized to highlight the relative peak positions.

Having identified a fluorophore whose photophysical properties are highly responsive to the presence of β-sheet secondary structure, we examined whether or not dapoxyl interacts with amyloid fibrils of the peptide hormone insulin, which are characterized by β-sheets aligned along the fibril axis.[1] The mechanism of aggregation of insulin has been explored in great detail in recent years.[42−45] In Figure 3C, we show that dapoxyl exhibits an intense peak in the presence of mature insulin amyloid fibrils, with an excitation maximum ($\lambda_{ex,max}$) of 370 nm and an emission maximum ($\lambda_{em,max}$) of 511 nm. As shown in Figure 3A,B, when dapoxyl interacts with the β-sheet form of K1, $\lambda_{ex,max}$ is 360 nm and $\lambda_{em,max}$ is 509 nm; with K2, $\lambda_{ex,max}$ is 368 nm and $\lambda_{em,max}$ is 479 nm. Hence, the peak position for mature fibrils is close to that of the poly(amino acid) model systems, and reflects the hydrophilic and hydrophobic β-sheet structural elements presented in mature fibrils.

It is additionally intriguing that neither the hydrophilic β-sheet nor the hydrophobic structural model, as shown for the β-sheet form of K1 in Figure 1C, was found to interact with ThT. This finding suggests that dapoxyl may be a more general probe of β-sheet structure than ThT. We were preliminarily intrigued by the possibility that dapoxyl may be able to detect aggregation intermediates that are not sufficiently structured to bind significantly to ThT. In order to avoid biasing the species observed toward those whose interactions are strong and persistent enough to be detected with *ex situ* assays, which involve dilution steps and a limited time resolution, we explored whether or not accurate *in situ* detection was possible by assessing whether or not dapoxyl affected the insulin aggregation kinetics. Bovine insulin solutions of varying concentrations were incubated in 50 mM NaCl at pH 2 under quiescent conditions, and formation of fibrils was monitored via an increase in ThT fluorescence intensity.

To explore whether or not dapoxyl affects the insulin aggregation mechanism, we compared directly the ThT kinetic traces observed for samples with and without dapoxyl. Kinetic traces for two representative protein concentrations are shown in Figure 4a. Consistently, the presence of dapoxyl did not affect the shape of the kinetic traces, suggesting that it does not affect the aggregation mechanism. We additionally examined the aggregation half times ($t_{1/2}$), at which half of the free monomer has been converted into aggregated material, and determined their scaling with monomer concentration as a means of defining the mechanism of aggregation.[46−49] As shown in Figure 4b, the presence of dapoxyl had no effect on the half-times at each of the protein concentrations examined, providing further confirmation that dapoxyl does not affect the mechanism of insulin aggregation and indicating that *in situ* aggregation assays are possible.

Accordingly, we were then able to perform a variety of *in situ* aggregation assays, which were time-resolved versions of the three-dimensional experiments reported in Figures 1b,c and 3. Monomer concentrations varied between 0.125 and 2.0 mg/mL, with and without the addition of preformed fibrils to seed the reaction, and buffer strengths varied between 10 and 50 mM NaCl. Three-dimensional fluorescence spectra were acquired at time points varying between 40 s and 10 min, depending on the experiment. Generally each condition was explored with a minimum of three replicate experiments.

Plots showing the results for the reactions under these conditions are given in the Supporting Information. To highlight the additional information gained from these multidimensional kinetic experiments, Figure 5a shows the

DOI: 10.1021/acs.jpcb.5b09663
J. Phys. Chem. B 2016, 120, 2087−2094

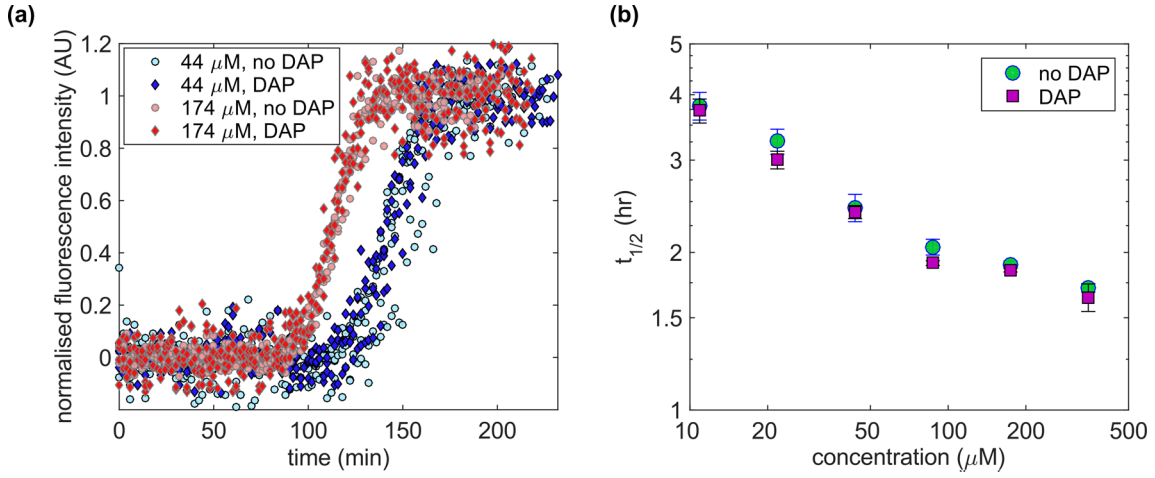

Figure 4. Dapoxyl does not affect the kinetics and mechanism of insulin aggregation. (a) Aggregation kinetic traces showing that the formation of mature fibrils is not perturbed by the presence of dapoxyl. Curves with and without dapoxyl are shown for two representative concentrations: 44 and 174 μM. (b) Half-times for the aggregation reactions ($t_{1/2}$) are highly similar with and without dapoxyl. The data are plotted on a log−log scale.

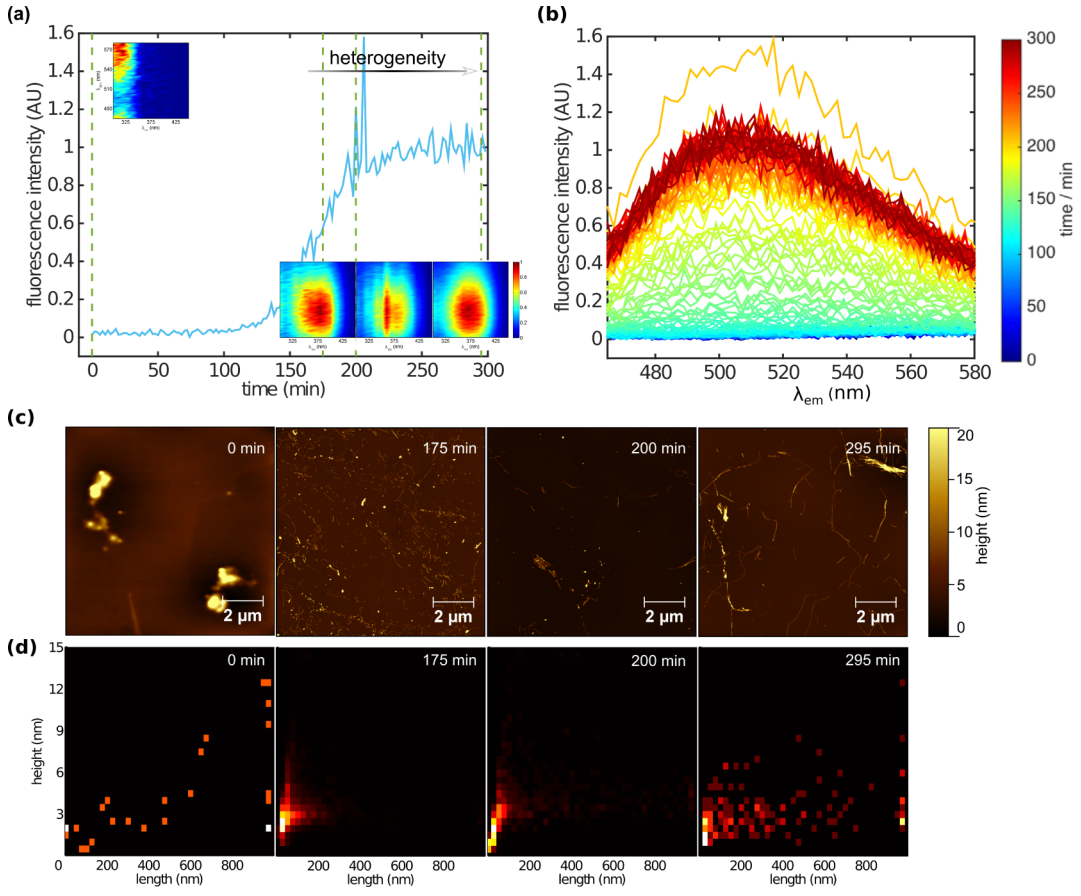

Figure 5. Characterization of the species formed during the aggregation reaction. 0.25 mg/mL bovine insulin was incubated at pH 2 in 50 mM NaCl and 60 °C, under quiescent conditions. To highlight the additional information gained with the methods described here, a "standard" kinetic trace is plotted monitoring the change in fluorescence intensity as a function of time when λ_{ex} = 360 nm and λ_{em} = 519 nm (a). Another dimension of information is added in (b), where the change in solvatochromic emission spectra is plotted as a function of time (indicated colorimetrically), with a constant excitation wavelength of 360 nm. The full three-dimensional spectra are plotted in Supporting Information Figure 5. An analogous aggregation reaction was monitored in real time as spectra were acquired, and aliquots were removed at time points (green dashed lines, (a)) whose spectra reveal the presence of aggregation intermediates. Normalized three-dimensional spectra for these time points are shown in (a). Representative AFM images are shown in (c). To generate the height/length plots (d), the features from generally between three and five images were identified and analyzed.

result obtained when the fluorescence intensity of dapoxyl is plotted as a function of time at a single excitation and emission wavelength, and Figure 5b shows the emission spectra of dapoxyl measured as a function of time at a constant excitation

DOI: 10.1021/acs.jpcb.5b09663
J. Phys. Chem. B 2016, 120, 2087−2094

wavelength. For reference, a representative one-dimensional kinetic trace using ThT fluorescence as a readout for an identical aggregation reaction is shown in Supporting Information Figure 4. Similar kinetics were observed with both probes.

A consistent finding was that dapoxyl does not interact with monomeric insulin but does interact with mature amyloid fibrils; indeed, differences in excitation spectra, emission spectra, and fluorescence intensity were observed during the aggregation reactions. Additionally, a number of intermediate peaks were detected in a concentration-dependent manner. The peaks were narrower than that observed for mature fibrils. When analogous three-dimensional aggregation experiments were set up using ThT as the fluorescent probe (Supporting Information Figure 6), ThT binding to mature insulin amyloid fibrils was observed with kinetics consistent with the appearance of the dapoxyl peaks characteristic of mature fibrils, but no intermediate peaks were detected. These data suggest that dapoxyl interacts with transient aggregation intermediates that are undetectable using conventional probes. Interestingly, we sometimes observe two peaks (for example, in Supporting Information Figure 5). We believe this to be an effect of the well-known heterogeneity of aggregating systems at intermediate time scales. Connecting these spectra to structures is the subject of ongoing work.

To begin to investigate the species giving rise to these peaks, additional experiments were performed in which aliquots of the reaction mixture were removed at time points where the spectra suggested that monomer, aggregation intermediates, or mature fibrils were present (Figure 5a). These aliquots were immediately deposited onto freshly cleaved mica surfaces, and atomic force microscopy (AFM) images were acquired. For each time point, at least three surfaces were prepared and imaged.

At the start of the aggregation reaction, the monomeric form of the protein is the only species present. The self-normalized three-dimensional fluorescence spectrum is analogous to that of dapoxyl alone or in the presence of species with which it does not interact (Figure 1c). Previous work has indicated that the drying process can stimulate the formation on the mica surface of the types of large, heterogeneous clumps of monomeric protein seen in Figure 5c, which have variable height and length distributions.

In the spectrum recorded after 175 min of aggregation, a new, broad peak, centered at $\lambda_{ex,max}$ of 380 nm and $\lambda_{em,max}$ of 505 nm, is evident in the fluorescence spectra and appears as though it could be a composite of several, more distinct peaks. The species generally have average heights between 2 and 3 nm, and average lengths of under 50 nm, though a broad distribution is observed (Figure 5d); this observation is consistent with the heterogeneous AFM images, which contain short fibrils and oligomers of varying morphologies, diameters, and association states.

In the spectrum recorded at 200 min, a more well-defined peak is observed, centered at $\lambda_{ex,max}$ of 360 nm and $\lambda_{em,max}$ of 500 nm. The AFM image reveals many short, thin fibrillar structures, as well as spherical oligomers and a minority of longer, thicker fibrils. Some oligomers are observed to be bound to the surface of fibrils and protofibrils; surface catalyzed secondary nucleation is not believed to be a dominant process in the mechanism of aggregation of insulin under the conditions used here,[50] so this observation could reflect the increased hydrophobicity of these species. These findings are distinct from the results observed for the sample imaged at 295 min, after the aggregation reaction had reached completion. Then, a peak consistent with the interaction of dapoxyl with mature fibrils is observed in the 3D fluorescence spectrum, with $\lambda_{ex,max}$ of 370 nm and $\lambda_{em,max}$ of 510 nm. A broad length distribution is seen, with a significant proportion of fibrils with lengths in excess of 1 μm.

The three-dimensional spectra and AFM images capture the heterogeneity expected for aggregating systems at intermediate time points. On the basis of the results of the poly(amino acid) model systems shown in Figures 1 and 3, these aggregation intermediates should be rich in β-sheet secondary structure. The $\lambda_{em,max}$ of the intermediates and fibrils varies somewhat, between 500 and 510 nm, while the intermediates are predominantly defined by differences in $\lambda_{ex,max}$, which varies between 360 and 380 nm. This result indicates, as shown in Figure 2, that for cases in which $\lambda_{ex,max}$ is shifted to higher energies the local solvent sphere either stabilizes the ground state more effectively or stabilizes the first excited state less efficiently, through differences in micropolarity or hydrogen bonding ability associated with binding to protein surfaces with different local secondary structure and hydrophobicity.

Increases in fluorescence intensity are expected to correlate with increases in local solvent sphere viscosity; when the dapoxyl molecule is more tightly bound to the protein interface, and more conformationally restricted as expected when binding takes place to highly ordered protein structures, nonradiative decay pathways become less significant and the fluorescence intensity is increased. We conclude that these spectroscopic changes, observed when dapoxyl interacts with species in this amyloid aggregation reaction, correspond to interactions with β-sheet-rich aggregates of varying hydrophobicity and compactness.

CONCLUSIONS

A variety of methods has been developed to monitor protein aggregation and the formation of amyloid fibrils. The ThT fluorescence assay, which monitors fibril abundance through an increase in the fluorescence intensity of a dye molecule that binds noncovalently to cross β-sheet structures,[8,9] is widely used. Increasing evidence suggests, however, that aggregation intermediates, which do not interact strongly with ThT,[12−14] are responsible for toxicity in amyloid aggregation reactions.[1] It has proved to be challenging, however, to monitor the evolution of these intermediate species with sufficient time resolution under representative biological conditions.[2] Accordingly, much effort has been expended in the study of isolated, stabilized populations of oligomers, and such studies have revealed that β-sheet-rich, frequently hydrophobic, conformational motifs are associated with aggregate toxicity.[3−7] It has been unclear, however, whether or not similar intermediate populations are observed for aggregation occurring under native conditions.

In the present study we have used model systems of poly(amino acid)s, which can adopt under defined conditions, well-defined variations in secondary structure, solvation, and hydrophobicity. We have used this model system to identify a fluorescent dye, dapoxyl, which exhibits dramatic changes in its excitation, emission, and fluorescence intensity in the presence of β-sheet-rich and hydrophobic conformational motifs, which have been associated with aggregate toxicity.[3−7] We have shown that dapoxyl interacts with mature insulin amyloid fibrils and that it does not affect the mechanism of insulin

DOI: 10.1021/acs.jpcb.5b09663
J. Phys. Chem. B 2016, 120, 2087−2094

aggregation. Moreover, we have explored the potential of using dapoxyl in monitoring the formation of mature fibrils and intermediates in an insulin aggregation reaction. Multiple peaks were observed and were defined primarily by variations in $\lambda_{ex,max}$ and fluorescence intensity that can be attributed to changes in the hydrophobicity and compactness of the dye binding site. Finally, the spectra were used to guide the characterization of aggregation intermediates with atomic force microscopy. Such species were found to differ in height and length from that of mature insulin fibrils. The results of these experiments suggest that conformationally sensitive fluorescent dyes, such as dapoxyl, represent a new and powerful tool for the extraction of detailed, time-resolved information about the changes in secondary structure and hydrophobicity that characterize the formation of intermediates in amyloid aggregation reactions and can indeed be used to detect key components of toxic aggregates.

■ ASSOCIATED CONTENT

Supporting Information

The Supporting Information is available free of charge on the ACS Publications website at DOI: 10.1021/acs.jpcb.5b09663.

Establishment of the poly(amino acid) model system, evaluation of other solvatochromic dyes, and multi-dimensional aggregation experiments performed under a variety of conditions (PDF)

■ AUTHOR INFORMATION

Corresponding Authors

*E-mail tpjk2@cam.ac.uk; phone +44 (0)1223 336344 (T.P.J.K.).

*E-mail cmd44@cam.ac.uk; phone +44 (0)1223 336344 (C.M.D.).

Notes

The authors declare no competing financial interest.

■ ACKNOWLEDGMENTS

The authors acknowledge the European Research Council (ERC), Biotechnology and Biological Sciences Research Council (BBSRC), Wellcome Trust, and Winston Churchill Foundation for financial support.

■ REFERENCES

(1) Chiti, F.; Dobson, C. M. Protein Misfolding, Functional Amyloid, and Human Disease. *Annu. Rev. Biochem.* **2006**, *75*, 333−366.

(2) Brorsson, A.-C.; Kumita, J. R.; MacLeod, I.; Bolognesi, B.; Speretta, E.; Luheshi, L. M.; Knowles, T. P. J.; Dobson, C. M.; Crowther, D. C. Methods and Models in Neurodegenerative and Systemic Protein Aggregation Diseases. *Front. Biosci., Landmark Ed.* **2010**, *15*, 373−396.

(3) Campioni, S.; Mannini, B.; Zampagni, M.; Pensalfini, A.; Parrini, C.; Evangelisti, E.; Relini, A.; Stefani, M.; Dobson, C. M.; Cecchi, C.; et al. A Causitive Link Between the Structure of Aberrant Protein Oligomers and Their Toxicity. *Nat. Chem. Biol.* **2010**, *6*, 140−147.

(4) Sandberg, A.; Luheshi, L. M.; Sollvander, S.; de Barros, T. P.; Macao, B.; Knowles, T. P. J.; Biverstal, H.; Lendel, C.; Ekholm-Petterson, F.; Dubnovitsky, A.; et al. Stabilization of Neurotoxic Alzheimer Amyloid-β Oligomers by Protein Engineering. *Proc. Natl. Acad. Sci. U. S. A.* **2010**, *107*, 15595−15600.

(5) Zampagni, M.; Cascella, R.; Casamenti, F.; Grossi, C.; Evangelisti, E.; Wright, D.; Becatti, M.; Liguri, G.; Mannini, B.; Campioni, S.; et al. A Comparison of the Biochemical Modifications Caused by Toxic and Non-Toxic Protein Oligomers in Cells. *Journal of Cellular and Molecular Medicine* **2011**, *15*, 2106−2116.

(6) Evangelisti, E.; Cecchi, C.; Cascella, R.; Sgromo, C.; Becatti, M.; Dobson, C. M.; Chiti, F.; Stefani, M. Membrane Lipid Composition and Its Physiochemical Properties Define Cell Vulnerability to Aberrant Protein Oligomers. *J. Cell Sci.* **2012**, *125*, 2416−2427.

(7) Cremades, N.; Cohen, S. I. A.; Deas, E.; Abramov, A. Y.; Chen, A. Y.; Orte, A.; Sandal, M.; Clarke, R. W.; Dunne, P.; Aprile, F. A.; et al. Direct Observation of the Interconversion of Normal and Toxic Forms of α-Synuclein. *Cell* **2012**, *149*, 1048−1059.

(8) LeVine, H. Thio avine T Interaction with Synthetic Alzheimer's Disease β-Amyloid Peptides: Detection of Amyloid Aggregation in Solution. *Protein Sci.* **1993**, *2*, 404−410.

(9) LeVine, H. Quantification of Beta-Sheet Amyloid Fibril Structures with Thioflavin T. *Methods Enzymol.* **1999**, *309*, 274−284.

(10) Khurana, R.; Coleman, C.; Ionescu-Zanetti, C.; Carter, S. A.; Krishna, V.; Grover, R. K.; Roy, R.; Sing, S. Mechanism of Thioflavin T Binding to Amyloid Fibrils. *J. Struct. Biol.* **2005**, *151*, 229−238.

(11) Biancalana, M.; Koide, S. Molecular Mechanism of Thioflavin-T Binding to Amyloid Fibrils. *Biochim. Biophys. Acta, Proteins Proteomics* **2010**, *1804*, 1405−1412.

(12) Walsh, D. M.; Hartley, D. M.; Kusumoto, Y.; Fezoui, Y.; Condron, M. C.; Lomakin, A.; Benedek, G. B.; Selkoe, D. J.; Teplow, D. B. Amyloid β-Protein Fibrillogenesis: Structure and Biological Activity of Protofibrillar Intermediates. *J. Biol. Chem.* **1999**, *274*, 25945−25952.

(13) Maezawa, I.; Hong, H.-S.; Liu, R.; Wu, C.-Y.; Cheng, R. H.; Kung, M.-P.; Kung, H. F.; Lam, K. S.; Oddo, S.; LaFerla, F. M.; et al. Congo Red and Thioflavin-T Analogs Detect Aβ Oligomers. *J. Neurochem.* **2008**, *104*, 457−468.

(14) Giehm, L.; Svergun, D. I.; Otzen, D. E.; Vestergaard, B. Low-Resolution Structure of a Vesicle Disrupting α-Synuclein Oligomer That Accumulates During Fibrillation. *Proc. Natl. Acad. Sci. U. S. A.* **2011**, *108*, 3246−3251.

(15) Nilsson, K. P. R.; Herland, A.; Hammarström, P.; Inganäs, O. Conjugated Polyelectrolytes: Conformation-Sensitive Optical Probes for Detection of Amyloid Fibril Formation. *Biochemistry* **2005**, *44*, 3718−3724.

(16) Herland, A.; Nilsson, K. P. R.; Olsson, J. D. M.; Hammarström, P.; Konradsson, P.; Inganäs, O. Synthesis of a Regioregular Zwitterionic Conjugated Oligoelectrolyte, Usable As an Optical Probe for Detection of Amyloid Fibril Formation at Acidic pH. *J. Am. Chem. Soc.* **2005**, *127*, 2317−2323.

(17) Nilsson, K. P. R.; Hammarström, P.; Ahlgren, F.; Herland, A.; Schnell, E. A.; Lindgren, M.; Westermark, G. T.; Inganäs, O. Conjugated Polyelectrolytes−Conformation-Sensitive Optical Probes for Staining and Characterization of Amyloid Deposits. *ChemBioChem* **2006**, *7*, 1096−1104.

(18) Nilsson, K. P. R.; Ikenberg, K.; Åslund, A.; Fransson, S.; Konradsson, P.; Röcken, C.; Moch, H.; Aguzzi, A. Structural Typing of Systemic Amyloidoses by Luminescent-Conjugated Polymer Spectroscopy. *Am. J. Pathol.* **2010**, *176*, 563−574.

(19) Fändrich, M.; Dobson, C. M. The Behaviour of Polyamino Acids Reveals an Inverse Side Chain Effect in Amyloid Structure Formation. *EMBO J.* **2002**, *21*, 5682−5690.

(20) Necas, D.; Klapetek, P. *Gwyddion: An Open-Source Software for SPM Data Analysis.* **2012**, *10*, 181−188.

(21) Otsu, N. *A Threshold Selection Method From Gray-Level Histograms* **1979**, *9*, 62−66.

(22) Tiffany, M. L.; Krimm, S. Effect of Temperature On the Circular Dichroism Spectra of Polypeptides in the Extended State. *Biopolymers* **1972**, *11*, 2309−2316.

(23) Rucker, A. L.; Creamer, T. P. Polyproline II Helical Structure in Protein Unfolded States: Lysine Peptides Revisited. *Protein Sci.* **2002**, *11*, 980−985.

(24) Greenfield, N. J. Using Circular Dichroism Spectra to Estimate Protein Secondary Structure. *Nat. Methods* **2006**, *6*, 2876−2890.

(25) Greenfield, N. J.; Fasman, G. D. Computed Circular Dichroism Spectra for the Evaluation of Protein Conformation. *Biochemistry* **1969**, *8*, 4108−4116.

DOI: 10.1021/acs.jpcb.5b09663
J. Phys. Chem. B 2016, 120, 2087−2094

(26) Squires, A. M.; Devlin, G. L.; Gras, S. L.; Tickler, A. K.; MacPhee, C. E.; Dobson, C. M. X-Ray Scattering Study of the Effect of Hydration On the Cross-β Structure of Amyloid Fibrils. *J. Am. Chem. Soc.* **2006**, *128*, 11738−11739.
(27) Gray, R. A.; Vander Velde, D. G.; Burke, C. J.; Manning, M. C.; Middaugh, C. R.; Borchardt, R. T. Delta-Sleep-Inducing Peptide: Solution Conformational Studies of a Membrane-Permeable Peptide. *Biochemistry* **1994**, *33*, 1323−1331.
(28) Chittchang, M.; Alur, H. H.; Mitra, A. K.; Johnston, T. P. Poly(L-Lysine) As a Model Drug Macromolecule with Which to Investigate Secondary Structure and Membrane Transport, Part I: Physicochemical and Stability Studies. *J. Pharm. Pharmacol.* **2002**, *54*, 315−323.
(29) Blout, E. R.; Lenormant, H. Reversible Configurational Changes in Poly-L-Lysine Hydrochloride Induced by Water. *Nature* **1957**, *179*, 960−963.
(30) Peggion, E.; Verdini, A. S.; cosani, A.; Scoffone, E. Conformational Studies On Polypeptides. Circular Dichroism Properties of Random Copolymers of Lysine and Phenylalanine in Aqueous Solutions at Various pH Values. *Macromolecules* **1970**, *3*, 194−198.
(31) Seipke, G.; Arfmann, H.-A.; Wagner, K. G. Synthesis and Properties of Alternating Poly(Lys-Phe) and Comparison with the Random Copolymer Poly(Lys51, Phe49). *Biopolymers* **1974**, *13*, 1621−1633.
(32) Milián, B.; Ortí, E.; Hernández, V.; López Navarrete, J. T.; Otsubo, T. Spectroscopic and Theoretical Study of Push-Pull Chromophores Containing Thiophene-Based Quinonoid Structures As Electron Spacers. *J. Phys. Chem. B* **2003**, *107*, 12175−12183.
(33) Reichardt, C. Solvatochromic Dyes As Solvent Polarity Indicators. *Chem. Rev.* **1994**, *94*, 2319−2358.
(34) Jablonski, A. Efficiency of Anti-Stokes Fluorescence in Dyes. *Nature* **1933**, *131*, 839−840.
(35) Franck, J.; Dymond, E. G. Elementary Processes of Photochemical Reactions. *Trans. Faraday Soc.* **1926**, *21*, 536−542.
(36) Condon, E. U. Nuclear Motions Associated with Electron Transitions in Diatomic Molecules. *Phys. Rev.* **1928**, *32*, 858−872.
(37) Loving, G. S.; Sainlos, M.; Imperiali, B. Monitoring Protein Interactions and Dynamics with Solvatochromic Fluorophores. *Trends Biotechnol.* **2010**, *28*, 73−83.
(38) Diwu, Z.; Zhang, C.; Klaubert, K. H.; Haugland, R. P. Fluorescent Molecular Probes VI. The Spectral Properties and Potential Biological Applications of Water-Soluble Dapoxyl Sulfonic Acid. *J. Photochem. Photobiol., A* **2000**, *131*, 95−100.
(39) Willets, K. A.; Callis, P. R.; Moerner, W. E. Experimental and Theoretical Investigations of Environmentally Sensitive Single-Molecule Fluorophores. *J. Phys. Chem. B* **2004**, *108*, 10465−10473.
(40) Grabowski, Z. R.; Rotkiewicz, K.; Rettig, W. Structural Changes Accompanying Intramolecular Electron Transfer: Focus On Twisted Intramolecular Charge-Transfer States and Structures. *Chem. Rev.* **2003**, *103*, 3899−4032.
(41) Lord, S. J.; Conley, N. R.; Lee, H.-l. D.; Nishimura, S. Y.; Pomerantz, A. K.; Willets, K. A.; Lu, Z.; Wang, H.; Liu, N.; Samuel, R.; et al. DCDHF Fluorophores for Single-Molecule Imaging in Cells. *ChemPhysChem* **2009**, *10*, 55−65.
(42) Ivanova, M. I.; Sievers, S. A.; Sawaya, M. R.; Wall, J. S.; Eisenberg, D. Molecular Basis for Insulin Fibril Assembly. *Proc. Natl. Acad. Sci. U. S. A.* **2009**, *106*, 18990−18995.
(43) Jiménez, J.; Nettleton, E. J.; Bouchard, M.; Robinson, C. V.; Dobson, C. M.; Saibil, H. R. The Protofilament Structure of Insulin Amyloid Fibrils. *Proc. Natl. Acad. Sci. U. S. A.* **2002**, *99*, 9196−9201.
(44) Knowles, T. P. J.; Shu, W.; Devlin, G. L.; Meehan, S.; Auer, S.; Dobson, C. M.; Welland, M. E. Kinetics and Thermodynamics of Amyloid Formation From Direct Measurements of Fluctuations in Fibril Mass. *Proc. Natl. Acad. Sci. U. S. A.* **2007**, *104*, 10016−10021.
(45) Knowles, T. P. J.; White, D. A.; Abate, A. R.; Agresti, J. J.; Cohen, S. I. A.; Sperling, R. A.; De Genst, E. J.; Dobson, C. M.; Weitz, D. A. Observation of Spatial Propagation of Amyloid Assembly From Single Nuclei. *Proc. Natl. Acad. Sci. U. S. A.* **2011**, *108*, 14746−14751.
(46) Cohen, S. I. A.; Vendruscolo, M.; Welland, M. E.; Dobson, C. M.; Terentjev, E. M.; Knowles, T. P. J. Nucleated Polymerization with Secondary Pathways. I. Time Evolution of the Principle Moments. *J. Chem. Phys.* **2011**, *135*, 065105.
(47) Cohen, S. I. A.; Vendruscolo, M.; Dobson, C. M.; Knowles, T. P. J. Nucleated Polymerization with Secondary Pathways. II. Determination of Self-Consistent Solutions to Growth Processes Described by Non-Linear Master Equations. *J. Chem. Phys.* **2011**, *135*, 065106.
(48) Cohen, S. I. A.; Vendruscolo, M.; Dobson, C. M.; Knowles, T. P. J. From Macroscopic Measurements to Microscopic Mechanisms of Protein Aggregation. *J. Mol. Biol.* **2012**, *421*, 160−171.
(49) Meisl, G.; Yang, X.; Hellstrand, E.; Frohm, B.; Kirkegaard, J. B.; Cohen, S. I. A.; Dobson, C. M.; Linse, S.; Knowles, T. P. J. Differences in Nucleation Behavior Underlie the Contrasting Aggregation Kinetics of the Aβ-40 and Aβ-42 Peptides. *Proc. Natl. Acad. Sci. U. S. A.* **2014**, *111*, 9384.
(50) Knowles, T. P. J.; Waudby, C. A.; Devlin, G. L.; Aguzzi, A.; Vendruscolo, M.; Terentjev, E.; Welland, M. E.; Dobson, C. M. An Analytical Solution to the Kinetics of Breakable Filament Assembly. *Science* **2009**, *326*, 1533−1537.

DOI: 10.1021/acs.jpcb.5b09663
J. Phys. Chem. B 2016, 120, 2087−2094